Electronic Supplementary Material (ESI) for Journal of Materials Chemistry A.
This journal is © The Royal Society of Chemistry 2020

Supporting Information

Optimizing Electron Density of Nickel Sulfides Electrocatalysts through Sulfur Vacancy Engineering for Alkaline Hydrogen Evolution

Dongbo Jia, [1, a] *Lili Han,* [2, b] *Ying Li,* [a] *Wenjun He,* [a] *Caichi Liu,* [a] *Jun Zhang,* [a] *Cong Chen,* [a] *Hui Liu* [* a, b] *, Huolin L. Xin* [*b]

[†] School of Material Science and Engineering, Hebei University of Technology, Dingzigu Road 1, Tianjin 300130, P. R. China.

[‡] Department of Physics and Astronomy, University of California, Irvine, CA 92697, USA.

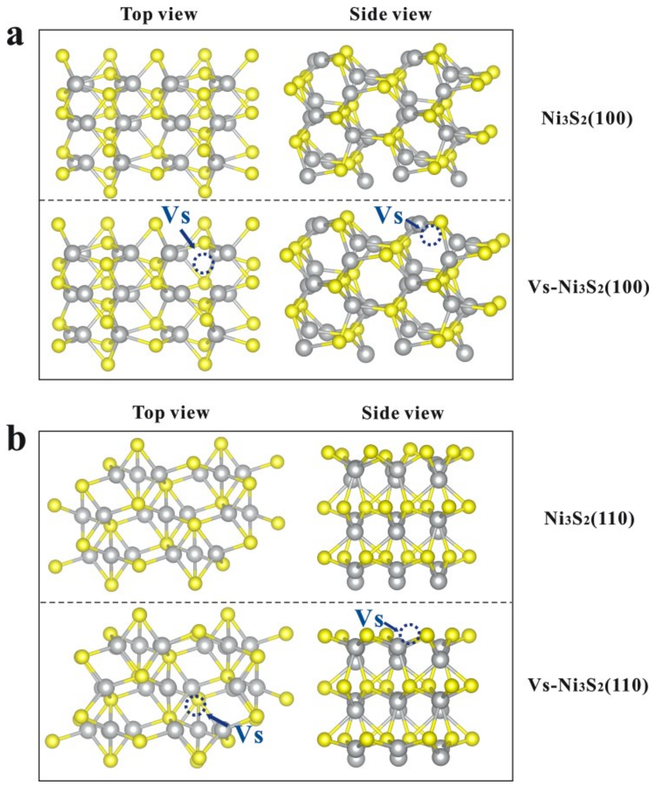

Figure S1. Top and side views on the (a) (100) and (b) (110) surface of Ni_3S_2 and Vs-Ni_3S_2. (Ni: gray; S: yellow)

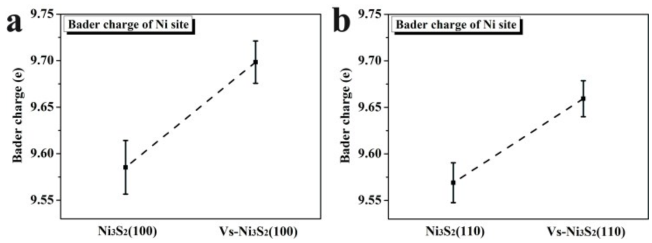

Figure S2. Bader charge analysis of the Ni sites around the S vacancies on (a) (100) and (b) (110) surfaces for the Vs-Ni_3S_2 and pristine Ni_3S_2.

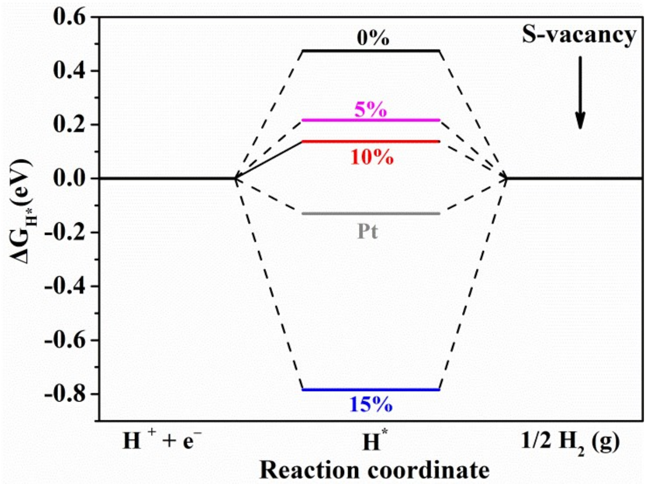

Figure S3. Gibbs free energies of hydrogen adsorption of Vs-Ni_3S_2/NF with different S-vacancy molar concentrations on (100) surfaces (X%= percentage of sulphur atoms removed in the model, such as 5%, 10%, 15%, respectively)

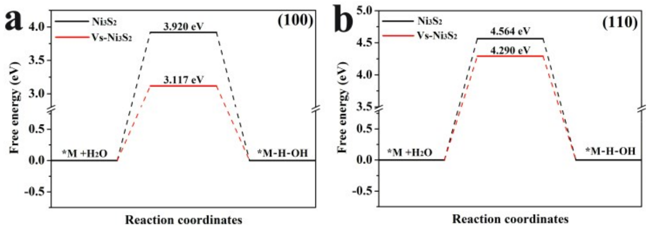

Figure S4. Free energy diagram of water dissociation on the (a) (100) and (b) (110) surface of Ni_3S_2 and Vs-Ni_3S_2.

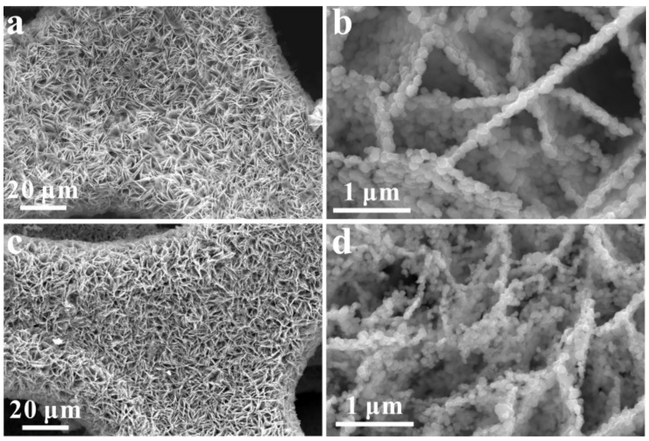

Figure S5. SEM image of (a, b) Vs-Ni_3S_2/NF-150, and (c, d) Vs-Ni_3S_2/NF-600.

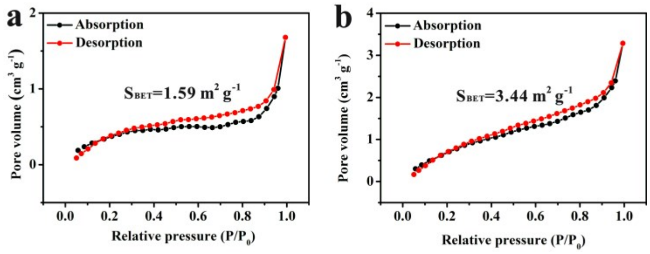

Figure S6. N_2 adsorption/desorption isotherm curves for Ni_3S_2/NF and (b) Vs-Ni_3S_2/NF.

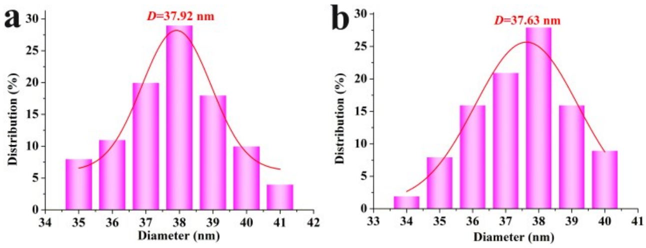

Figure S7. Particle size distribution diagram of (a) Ni_3S_2 nanoparticles on Ni_3S_2/NF and (b) Vs-Ni_3S_2 nanoparticles on Vs-Ni_3S_2/NF.

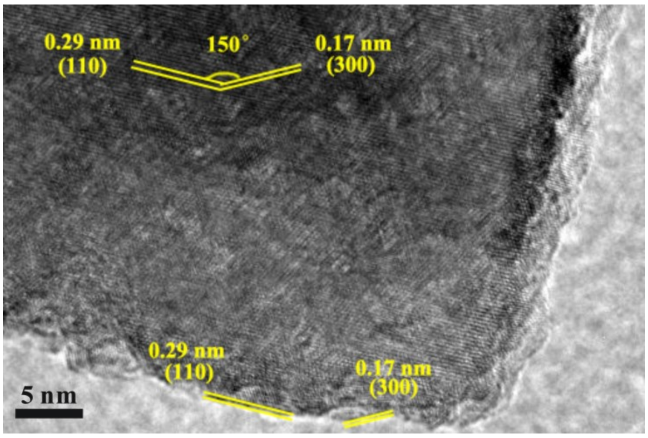

Figure S8. HRTEM image of the edge of Vs-Ni_3S_2/NF nanoplate.

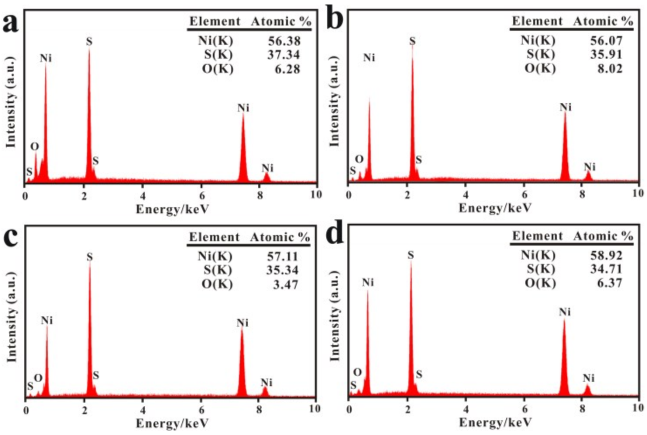

Figure S9. EDS spectrum of (a) Ni_3S_2/NF, (b) Vs-Ni_3S_2/NF-150, (c) Vs-Ni_3S_2/NF-300 and (d) Vs-Ni_3S_2/NF-600.

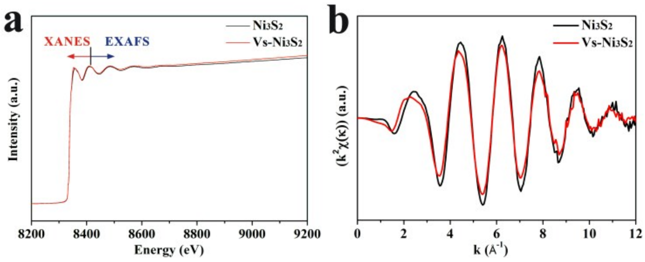

Figure S10. (a) Ni K-edge XAFS spectra of Ni_3S_2/NF and Vs-Ni_3S_2/NF, (b) corresponding oscillation curves $k^2\chi(\kappa)$.

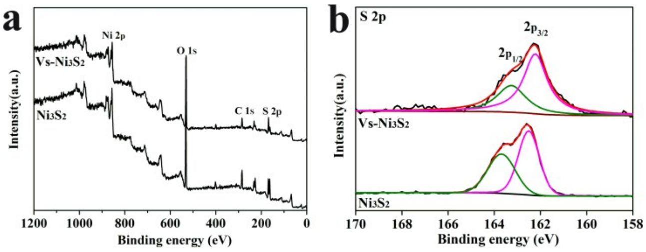

Figure S11. (a) XPS spectra of survey for Ni_3S_2/NF and Vs-Ni_3S_2/NF, (b) XPS spectra of S 2p for Ni_3S_2/NF and Vs-Ni_3S_2/NF.

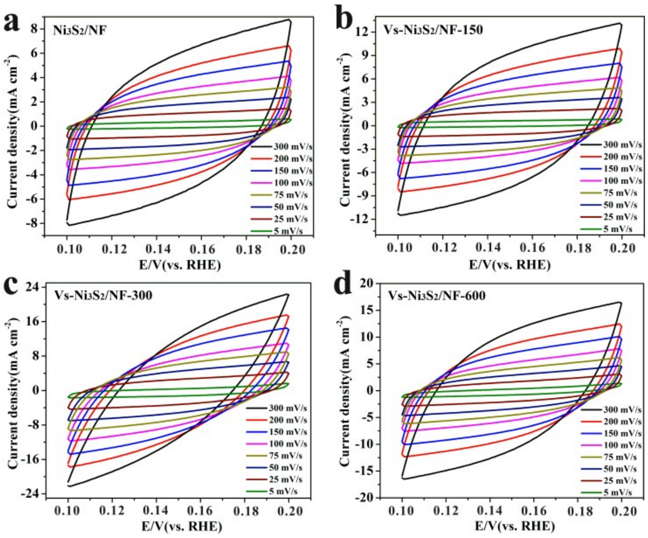

Figure S12. Typical cyclic voltammetry curves of Ni_3S_2/NF and Vs-Ni_3S_2/NF treated with different time.

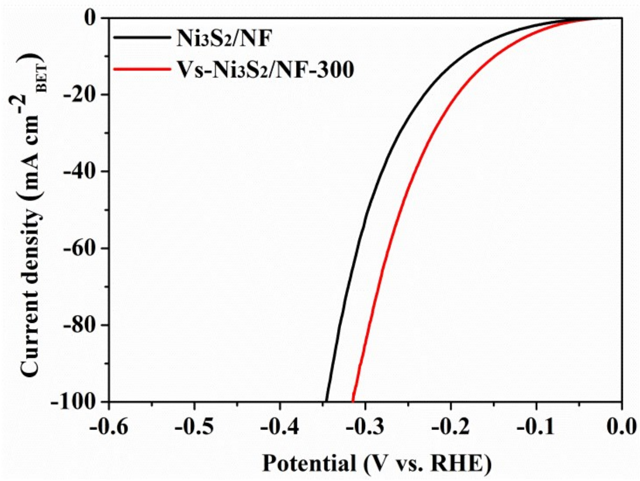

Figure S13. The specific activity of Ni_3S_2/NF and Vs-Ni_3S_2/NF based on the BET surface areas.

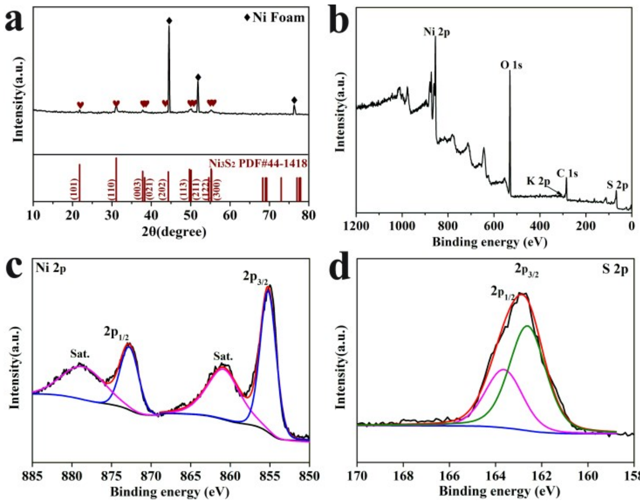

Figure S14. (a) XRD pattern, Survey (b), Ni 2p (c) and S 2p (d) XPS spectra of Vs-Ni_3S_2/NF after HER.

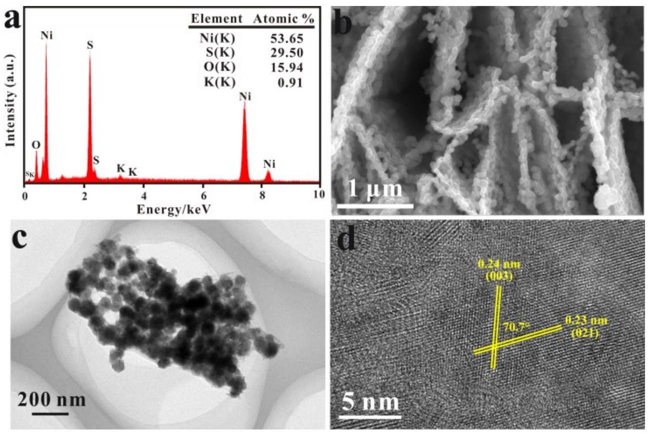

Figure S15. (a) EDS spectrum, (b) SEM, (c) TEM image and (d) HRTEM image of Vs-Ni_3S_2/NF after HER.

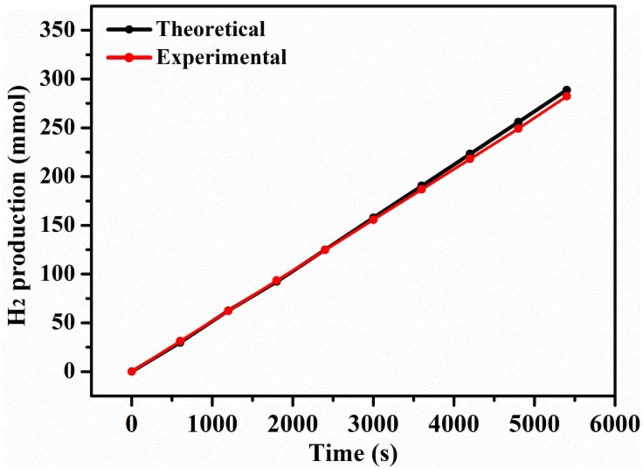

Figure S16. The theoretical (black line) and experimental (red curve) results of H_2 production on Vs-Ni_3S_2/NF electrode.

Table S1. Formation energy of S-vacancy on the (100) and (110) surface of Vs-Ni_3S_2.

Facet	(100)		(110)	
	Surface	Lattice	Surface	Lattice
Formation energy of S-vacancy (eV)	2.223	3.494	2.745	3.263

Table S2. ICP-AES data and the atomic ratio of Ni/S in different catalysts.

Samples	Concentration (mg L^{-1})		Atomic ratio of Ni/S (mol/mol)
	Ni	S	
Ni_3S_2/NF	14.73	5.39	105.98/71.13 (1.49/1)
Vs-Ni_3S_2/NF-150	14.49	5.03	104.26/66.41 (1.57/1)
Vs- Ni_3S_2/NF-300	14.22	4.73	102.32/62.39 (1.64/1)
Vs- Ni_3S_2/NF-600	13.86	4.39	99.70/57.97 (1.72/1)
Vs- Ni_3S_2/NF-300 after HER	14.15	4.59	101.84/60.62 (1.68/1)

Table S3. The loading amount of different catalysts.

Sample	Loading of catalyst (mg cm^{-2})					
	1	2	3	4	5	Average
Pt/C	--	--	--	--	--	2.92
Ni_3S_2/NF	3.06	2.90	3.02	2.93	2.99	2.98±0.06
Vs-Ni_3S_2/NF-150	3.02	2.96	3.01	2.88	2.93	2.96±0.05
Vs-Ni_3S_2/NF-300	2.85	2.95	2.91	2.98	2.91	2.92±0.04
Vs-Ni_3S_2/NF-600	2.86	2.76	2.92	2.93	2.88	2.87±0.06

Table S4. Comparison of the HER performance of Vs-Ni_3S_2/NF-300 with other well-performed electrocatalysts.

Catalysts	η@10 mA cm^{-2}	η@20 mA cm^{-2}	η@100 mA cm^{-2}	Tafel slope	Ref.
	mV	mV	mV	mV dec^{-1}	
Vs-Ni_3S_2/NF-300	88	120	218	87	This work
High-Index Faceted Ni_3S_2/NF	223	~300	--	--	1
(003)-Ni_3S_2 NFs	135	177	--	75.7	2
N-Ni_3S_2/NF	110	~160	~230	--	3
Sn-Ni_3S_2/NF	137	~200	~320	148	4
V-Ni_3S_2/NF	--	203	~350	112	5
Mn-Ni_3S_2/NF	152	--	--	98	6
$Fe_{17.5\%}$-Ni_3S_2/NF	47	142	232	95	7
$P_{9.03\%}$-$(Ni, Fe)_3S_2$/NF	98	135	218	88	8

$Ni_xCo_{3-x}S_4/Ni_3S_2/NF$	136	--	258	107	[9]
Cu NDs-Ni_3S_2 NTs	128	~160	~270	76.2	[10]
Ni-Ni_3S_2-2	114	155	--	122	[11]

Table S5. EIS results of Ni_3S_2/NF and Vs-Ni_3S_2/NF treated with different time.

	Ni_3S_2/NF	Vs-Ni_3S_2/NF-150	Vs-Ni_3S_2/NF-300	Vs-Ni_3S_2/NF-600
$R_s[\Omega]$	1.62	1.64	1.59	1.66
$R_{ct}[\Omega]$	3.98	3.3	2.26	2.47

REFERENCES

(1) Feng, L. L.; Yu, G.; Wu, Y.; Li, G. D.; Li, H.; Sun, Y.; Asefa, T.; Chen, W.; Zou, X. High-Index Faceted Ni_3S_2 Nanosheet Arrays as Highly Active and Ultrastable Electrocatalysts for Water Splitting. *J Am. Chem. Soc.* **2015,** *137*, 14023-14026.

(2) Dong, J.; Zhang, F. Q.; Yang, Y.; Zhang, Y. B.; He, H.; Huang, X.; Fan, X.; Zhang, X. M. (003)-Facet-exposed Ni_3S_2 nanoporous thin films on nickel foil for efficient water splitting. *Appl. Catal. B* **2019,** *243*, 693-702.

(3) Chen, P.; Zhou, T.; Zhang, M.; Tong, Y.; Zhong, C.; Zhang, N.; Zhang, L.; Wu, C.; Xie, Y. 3D Nitrogen-Anion-Decorated Nickel Sulfides for Highly Efficient Overall Water Splitting. *Adv. Mater.* **2017,** *29*, 1701584.

(4) Yu, J.; Ma, F. X.; Du, Y.; Wang, P. P.; Xu, C. Y.; Zhen, L. In Situ Growth of Sn-Doped Ni_3S_2 Nanosheets on Ni Foam as High-Performance Electrocatalyst for Hydrogen Evolution Reaction. *Chemelectrochem* **2017,** *4*, 594-600.

(5) Qu, Y.; Yang, M.; Chai, J.; Tang, Z.; Shao, M.; Kwok, C. T.; Yang, M.; Wang, Z.; Chua, D.; Wang, S.; Lu, Z.; Pan, H. Facile Synthesis of Vanadium-Doped Ni_3S_2 Nanowire Arrays as Active Electrocatalyst for Hydrogen Evolution Reaction. *ACS Appl. Mater. Inter.* **2017,** *9*, 5959-5967.

(6) Du, H.; Kong, R.; Qu, F.; Lu, L. Enhanced electrocatalysis for alkaline hydrogen evolution by Mn doping in a Ni_3S_2 nanosheet array. *Chem. Commun.* **2018,** *54*, 10100-10103.

(7) Zhang, G.; Feng, Y.-S.; Lu, W. T.; He, D.; Wang, C. Y.; Li, Y. K.; Wang, X. Y.; Cao, F. F. Enhanced Catalysis of Electrochemical Overall Water Splitting in Alkaline Media by Fe Doping in Ni_3S_2 Nanosheet Arrays. *ACS Catal.* **2018,** *8*, 5431-5441.

(8) Liu, C.; Jia, D.; Hao, Q.; Zheng, X.; Li, Y.; Tang, C.; Liu, H.; Zhang, J.; Zheng, X. P-Doped Iron-Nickel Sulfide Nanosheet Arrays for Highly Efficient Overall Water Splitting. *ACS Appl. Mater. Inter.* **2019,** *11*, 27667-27676.

(9) Wu, Y.; Liu, Y.; Li, G. D.; Zou, X.; Lian, X.; Wang, D.; Sun, L.; Asefa, T.; Zou, X. Efficient electrocatalysis of overall water splitting by ultrasmall $NixCo_{3-x}S_4$ coupled Ni_3S_2 nanosheet arrays. *Nano Energy* **2017,** *35*, 161-170.

(10) Feng, J. X.; Wu, J. Q.; Tong, Y. X.; Li, G. R. Efficient Hydrogen Evolution on Cu Nanodots-Decorated Ni_3S_2 Nanotubes by Optimizing Atomic Hydrogen Adsorption and Desorption. *J. Am. Chem. Soc.* **2018,** *140*, 610-617.

(11) Zheng, X.; Peng, L.; Li, L.; Yang, N.; Yang, Y.; Li, J.; Wang, J.; Wei, Z. Role of non-metallic atoms in enhancing the catalytic activity of nickel-based compounds for hydrogen evolution reaction. *Chem. Sci.* **2018,** *9*, 1822-1830.